Characterizing the chemical composition of red coloring matter samples from the Altamira cave using synchrotron μXRF imaging

José Tapia, Myriam Eveno, Alfredo Prada, Pilar Fatás, Carmen de las Heras, Pablo Arias, Katharina Müller, Sebastian Schöder, Ina Reiche

Applied Physics A (2024) 130:813
https://doi.org/10.1007/s00339-024-07950-5

S.I.: SR2A - SYNCHROTRON RADIATION AND NEUTRONS IN ART AND ARCHAEOLOGY 2023

Characterizing the chemical composition of red coloring matter samples from the Altamira cave using synchrotron µXRF imaging

José Tapia[1,2] · Myriam Eveno[2,3] · Alfredo Prada[4] · Pilar Fatás[4] · Carmen de las Heras[4] · Pablo Arias[5] · Katharina Müller[6] · Sebastian Schöder[7] · Ina Reiche[1]

Received: 9 February 2024 / Accepted: 1 October 2024

Abstract
The chemical in situ study of red coloring matter from Paleolithic cave art is challenging because the same trace elements can be present both in the matter and in the calcitic support, and the two present a heterogeneous composition. In this study, thirteen red iron oxide-based coloring matter samples obtained at drip points coming from eight locations within the *Techo de los Polícromos*, Altamira cave (Spain), have been analyzed by highly sensitive synchrotron-induced micro-X-ray fluorescence (SR-µXRF). Our analyses improved the characterization of red Paleolithic pigments by establishing characteristic trace element patterns, additionally facilitating a comparison of the distinct representations within the cave. Furthermore, new differentiation criteria between the composition of the calcitic walls and that of the red coloring matter could be established, helping to improve future non-invasive analyses.

Keywords SR-µXRF · Elemental imaging · Paleolithic cave art · Red coloring matter · Iron oxides · Altamira cave

1 Introduction

Paleolithic cave art, being one of the earliest manifestations of artistic representations from modern humans, holds an important significance. In Europe, the Northern Spain and Southern France regions are home to most of this remarkable prehistoric art, with some caves like Altamira and La Garma in Spain, and Lascaux and Chauvet in France, designated UNESCO World Heritage Sites [1–7]. The paintings or drawings in these caverns depict predominantly animals and elements that were significant to the people living at that time. By studying these representations, the origins of human artistic expression, symbolism and cognitive development can be further explored [8, 9]. Specifically, analyzing the materials used in the creation of these artworks can provide insights into aspects such as the resource utilization, the selection and preparation of pigments, trade and exchange networks, and the technological progress of prehistoric societies.

The first physicochemical analyses of micro samples of coloring matter coming from prehistoric caves were performed at the beginning of the 20th century [9, 10]. During the 1970s and 80s, the caves of Altamira and Lascaux were subject to in-depth systematic analyses [11–13] that were extended to other cave sites in the following years. Since then, micro samples have been analyzed using a variety of different techniques in laboratories [3, 9, 14–17] and, more recently, at synchrotron facilities [14, 18, 19] and particle accelerators [15, 20]. In addition, measurements can also be carried out on site with portable devices without the need

✉ Ina Reiche
ina.reiche@culture.gouv.fr

1 Laboratoire de développement instrumental et de méthodologies innovantes pour les biens culturels (Lab-BC), CNRS - C2RMF - Chimie ParisTech Université PSL, UAR 3506, Paris 75001, France

2 PSL Research University, Chimie ParisTech - CNRS, IRCP, UMR 8247, Paris 75005, France

3 Centre de Recherche et de Restauration des Musées de France (C2RMF), Paris 75001, France

4 Museo Nacional y Centro de Investigación de Altamira, Santillana del Mar, Cantabria, Spain

5 Instituto Internacional de Investigaciones Prehistóricas de Cantabria (IIIPC), Universidad de Cantabria - Gobierno de Cantabria-Santander, Santander 39005, Spain

6 IPANEMA, CNRS - Ministère de la Culture (MC) - UVSQ - MNHN, UAR 3461, Gif-sur-Yvette 91192, France

7 Synchrotron SOLEIL, Saint-Aubin, Gif-sur-Yvette 91192, France

Published online: 21 October 2024

for sampling [10, 14, 18, 19]. For instance, in recent years X-ray Fluorescence spectroscopy (XRF) has proven to be an efficient, fast, non-invasive, and relatively safe method for measuring spots on artworks and obtaining information on elemental compositions [21], by means of an X-ray beam of small diameter and an energy dispersive detector [22, 23].

The color palette habitually used in Paleolithic representations consists of red and black, but can sometimes be extended to brown, yellow, purple, grey and white [9, 11, 24]. The coloring matter was usually broken down and milled, possibly mixed with a binder, and applied on the support [11, 24]. Reds, yellows and browns are generally ochres rich in iron (Fe) oxides (mainly hematite and goethite) [14–16, 20]. Blacks come from manganese (Mn) oxides or carbon black from burned the combustion of organic materials.

Black coloring matter based on Mn oxides has been well studied and characterized. Using samples from the Lascaux cave, Reiche et al. demonstrated that different phases can be identified with the aid of Scanning Electron Microscopy and Transmission Electron Microscopy coupled with an Energy Dispersive X-ray Spectroscopy system (SEM-EDX and TEM-EDX) [25]. Furthermore, trace elements like Ba and K can be used to obtain a chemical fingerprint [26, 27], as they are part of the oxide structure.

The in situ study of black coloring matter in caves is also possible with portable XRF (pXRF), as demonstrated in the Rouffignac cave by Gay et al. [6] and Beck et al. [28], but requires appropriate access to the representations as the measurements are time consuming. Moreover, this approach is not always feasible at cave sites due to logistical challenges, permission, and the delicate nature of the artworks.

The characterizing approaches developed for black coloring matter, unfortunately, cannot be applied to red Fe oxide-based matter. Since this red matter is generally hematite-based with a varying proportion of goethite calcite and earth charges, the search for characteristic phase differentiation criteria is complicated. In consequence, the strategy pursued is to search for distinct trace elements. However, further challenges arise with this approach, as some of the minor and trace elements can be present in both the red Fe oxide-based coloring matter and in its calcitic support, and the two present a heterogeneous composition.

The Altamira cave, situated in the region of Cantabria in Northern Spain, was one of the first prehistoric caves to be discovered, unearthed in 1879 by Marcelino Sanz de Sautuola. The cave is believed to have been frequented from 36.500 BP until 13.000 BP, when a landslide shut the entrance [29, 30]. Admired for its exquisite paintings, Altamira's significance lies not only in its remarkable preservation but also in the rich and complex polychrome decorations it presents, with the *Techo de los Polícromos* area (Polychrome Ceiling) standing out as an unparalleled masterpiece. This intricately painted chamber ceiling showcases a rich palette of reds, blacks, browns, yellows and purples, portraying an array of animals in dynamic motion, handprints and claviform signs, going to lengths such as using the rock's natural volume to enhance the contours of the animals and accentuate their lifelike appearance. Being one of the earliest and rarest examples of polychrome art in prehistory, Altamira has been fundamental in reshaping the understanding of Paleolithic artistic capabilities, showcasing the advanced skills our ancestors possessed in order to paint this "Sistine Chapel of the Upper Paleolithic" [30, 31].

In 1978, Cabrera Garrido et al. discovered that several samples of ochre fragments unearthed from the floor of the Altamira cave, which might have been used for painting some of its figures, contained variable amounts of calcium carbonates [11]. This element is usually also a major component of cave walls. As mentioned, some of the minor and trace elements can be present in both the red Fe oxide-based coloring matter and its calcitic support, with the two presenting a heterogeneous composition. Cabrera Garrido's results confirms this in the specific case of the Altamira cave, further complicating the analysis of the coloring matter.

To overcome these challenges and successfully characterize the red matter in cave art, various strategies can be employed. These include the use of confocal XRF (CXRF) [32], combining in situ pXRF with other microsample-based methods [19], or applying powerful data treatment strategies [33]. In this study, we opted for highly sensitive measurements performed at a synchrotron facility, which we identified as the most promising approach. Due to its high brilliance, synchrotron radiation (SR) allows for an enhancement of the elemental sensitivity in XRF analyses. Additionally, complex data evaluation techniques, including semi-quantitative data evaluation protocols [26] and statistical approaches [34–36], can be applied subsequently to further refine the accuracy of the results.

In the presented study, micrometric red-colored samples coming from the *Techo de los Polícromos* were examined using SR-μXRF. The aim was to characterize the chemical composition of the Fe-rich red coloring matter thanks to the high sensitivity of this technique and to find and confirm new markers in the form of characteristic minor and trace elements associated with the red matter. This study allows to finely compare the representations between them in the same cave, as will be shown here. Moreover, relations and possible explanations for the creation of different figures can be hypothesized based on these results. Additionally, different Paleolithic cave sites could be compared between them in a follow-up study, resulting in a larger picture of the use of red coloring matter on a regional scale during Paleolithic times in Northern Spain.

2 Materials and methods

2.1 Special conditions of the cave

The Altamira cave presents unique and challenging conditions for both preservation and study. Access is highly restricted, and permission to sample is exceedingly difficult to obtain, if not impossible, and must be avoided at all costs. When researchers or conservation teams are granted entry, they must adhere to strict time limits set by the Preventive Conservation Plan (PCP) of the cave. This plan, which is based on thorough diagnostics of the cave art's main alterations, establishes a series of actions and monitoring protocols.

These protocols define maximum stay times in the cave, referred as "workload", which is the time spent multiplied by the number of people present. Stay times are determined based on historical environmental studies, with reference values that have been rigorously applied since the implementation of the PCP. Parameters including CO_2 levels are rigorously monitored to ensure environmental stability. Such strict regulations aim to minimize human impact on the delicate environment.

The ceiling of the *Sala de los Polícromos* (Polychrome Hall), which was reinforced with artificial walls in the 20th century to prevent collapse, is particularly fragile and requires careful monitoring to prevent vibrations or disturbances. Consequently, and in line with the PCP, in situ analyses with portable instruments such as pXRF, were not feasible for our study.

2.2 Unique sampling method and sample preparation

Water naturally flows slowly from cracks in the ceiling of the *Sala de los Polícromos* due to gravity. In the areas where the cave ceiling is lower, the water droplets can remain and accumulate. When these small zones belong to a colored figure, the drops can erode and detach coloring matter from the support before dripping on the floor, bringing matter from precise locations on their way down [37]. CO_2 can also play an important role in these detachment processes, contributing to the creation of mildly acidic conditions that accelerate the erosion of the support and transport of the coloring matter [38].

By means of various glass containers and synthetic Tyvek® fabrics placed on the floor (Figs. 1b and 2b), these falling micrometric grains of coloring matter can be captured. The receptacles containing this matter are then examined in the laboratory using optical microscopy (OM, Fig. 2b). Samples of a few hundred micrometers of coloring matter are carefully selected, collected with a fine scalpel, and deposited on carbon tape, which holds them in position in the synchrotron's sample holder (Fig. 2c for sample

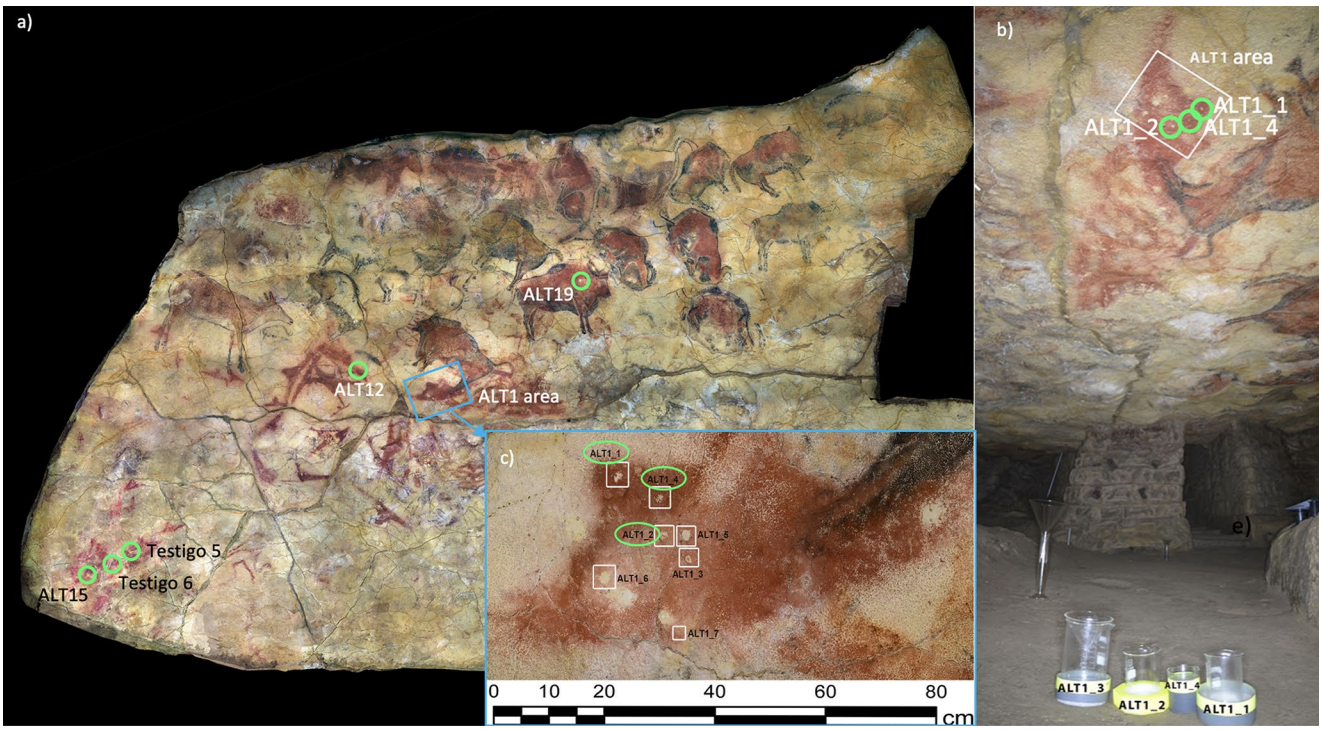

Fig. 1 a) *Techo de los Polícromos* (Polychrome Ceiling) in the *Sala de los Polícromos* (Polychrome Hall), with the studied drip points marked with a green circle, b) active drip area ALT1, with glass recipients positioned under it, c) zoom of the drip area ALT1, with drip points ALT1_1, ALT1_2 and ALT1_4 marked in green © Museo de Altamira, A. Prada / CNRS, J. Tapia

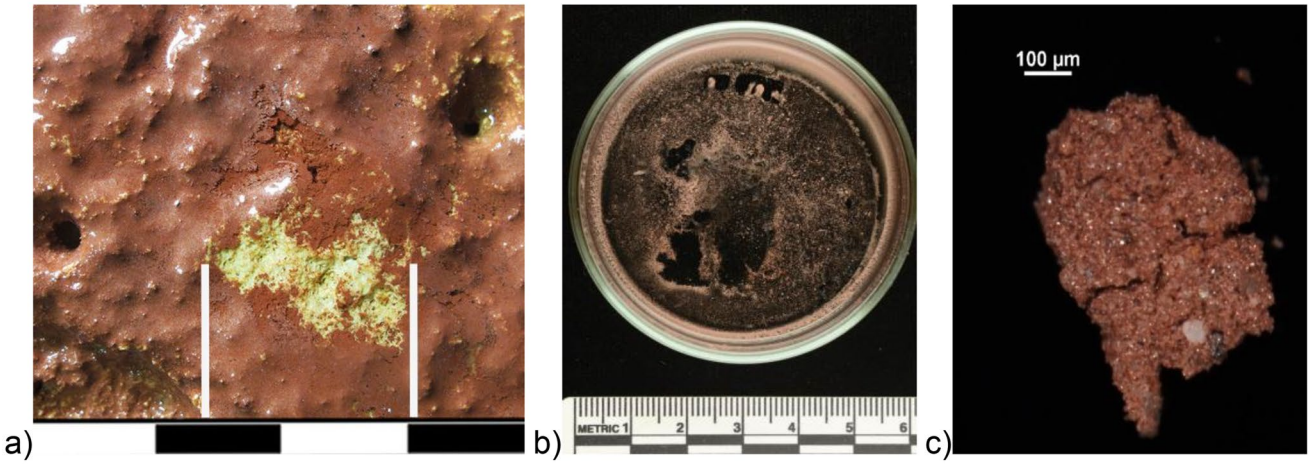

Fig. 2 **a**) Void of color in a claviform sign (drip point ALT1_2), **b**) glass receptacle with dried coloring matter grains at the bottom, **c**) optical image of sample ALT1_4 deposited on black carbon scotch © Museo de Altamira, A. Prada / CNRS J. Tapia

Table 1 Name of the thirteen studied samples, their cave figure and drip points provenance, and collection date

Sample	Representation	Drip point	Date of collection
ALT1_1A	Claviform sign A, in ALT1 area	ALT1_1	March 2021
ALT1_1B			March 2021
ALT1_1C			March 2021
ALT1_1			April 2021
ALT1_2	Claviform sign B?, in ALT1 area	ALT1_2	April 2021
ALT1_4	Superposition of claviform signs A and B, in ALT1 area	ALT1_4	June 2021
ALT12	Claviform sign C	ALT12	-
ALT12_3			May 2023
ALT12_4			April 2014
ALT15	Claviform sign D	ALT15	June 2022
ALT19	Polychrome bison	ALT19	March 2017
Testigo 5	Claviform sign E	-	May 2023
Testigo 6	Claviform sign F	-	June 2023

ALT1_4). The optical micrograph of the thirteen samples is provided in the SI.

Thirteen samples of coloring matter from eight different drip points belonging to seven different figures from the *Techo de los Polícromos* are presented in this study. Drip point ALT1_2 is shown in detail in Fig. 2a. Since the slow precipitation has been collected in periods lasting several years, more than one sample can exist for the same drip point. Twelve of the samples are red, originating from different claviform representations, while the thirteenth is a darker reddish-brown and comes from a bison figure. A map of the Polychrome Hall indicating the precise analyzed locations can be found in Fig. 1a.

Drip points ALT1_1, ALT1_2, ALT1_4, ALT12, ALT15, Testigo 5 and Testigo 6 correspond to various signs, and ALT19 to a polychrome bison. Four microsamples from drip point ALT1_1 were studied: three that fell in March 2021 (samples ALT1_1A, ALT1_1B and ALT1_1C), and one that fell in April 2021 (sample ALT1_1). Three samples from drip point ALT12 were also analyzed: one collected in April 2014 (sample ALT12_4), a second one in May 2023 (samples ALT12_3), and a third one without a date (sample ALT12). Table 1 lists all the samples, the representations to which they belong, the drip points from which they originate and their date of collection. The samples studied here are of high importance due to their rarity and their representativeness of different figures within the *Techo de los Polícromos* area of the cave.

Further images of the ALT1 area and the ALT19 drip points can be found in [37, 38].

2.3 Representativeness of the samples

The representativeness of the samples can, in fact, be questioned. Environmental factors affecting pigment adhesion in the Altamira cave, as well as the representativeness and origin of the collected coloring matter samples, are evaluated. Recently, Bayarri et al. [37, 38] conducted in-depth studies on pigment adhesion loss to the support in the Altamira cave, examining the effects of moisture and water presence, the role of CO_2 in detachment and entrainment processes, and the trajectory of water on the cave ceiling.

We have scrutinized potential discrepancies in the collection and representativeness of the studied coloring matter, elucidating several factors in the following lines.

We consider the colored droplets to have been falling for some time, following the same "stream routes" studied by Bayarri et al. [37, 38]. Going at a relative fast pace from the cracks to low altitude areas where they accumulate and linger, the risk of them transporting coloring matter along the way is low. Therefore, we hypothesize that the matter

dropping into the floor receptacles is mainly local, from where the droplets settle and detach the matter. Given that the red iron oxide is not soluble at the pH levels of 7–8 found in these water drops, as measured by a team member, it is assumed to remain intact while detaching from the ceiling. It is more likely the mechanical action of the fluids that make them fall down rather than a chemical dissolution [37–39].

Small fragments of calcitic support could also detach from these zones and carry coloring matter with them. These fragments can be easily distinguished from the red matter using an optical microscope. It could only be slightly found on two out of the thirteen here studied samples (ALT12_3 and Testigo 6, see SI).

The composition of the water drizzling through the cracks can be considered chemically unchanged, as in a scale of several meters neither the rain nor the earth over the cave's ceiling can be supposed strongly heterogeneous.

We can think of each of the studied red claviform signs as painted at a different time, with a unique preparation of coloring matter. As these abstract shapes are quite small and simple representations, the red matter should have a similar solubility in the seven locations concerning these six signs. The studied polychrome bison, with its different colors, could nevertheless have different coloring matters precipitating on the floor. Accepting these hypotheses, the main differences in coloring matter should then not be due to the water composition or its flowing, but rather to the different chemical composition of the matter present locally at the precipitation points in the small area surrounding the droplet formation.

A possible source of discrepancy between results from samples coming from the same drip point could come from the washing out of color over time, the first samples to fall likely having a higher concentration of coloring matter than the later ones. The slight heterogeneity of the coloring matter block at the microscale also needs to be considered. Controlled and experimental tests should follow this first study to verify that the collected samples are an accurate representation of the pigment composition on the cave ceiling.

2.4 Experimental conditions

2.4.1 Optical microscopy (OM)

The microsamples were examined using Optical Microscopy (OM) with various lighting and filters (visible, blue, and UV lights) on a Nikon Eclipse LV-100ND microscope equipped with a Nikon DS-Ri1 camera.

2.4.2 SR-XRD

X-ray Diffraction (XRD) measurements were performed on a sample from drip point ALT1_1 at the ID22 beamline of the European Radiation Synchrotron Facility (ESRF) within the Historical Materials Block Allocation Group (BAG) Access [40], making use of the high-brilliance available at this facility. The X-ray beam is highly collimated using a monochromator, ensuring precise diffraction studies. An accurate and precise diffractometer capable of accommodating spinning capillary or flat plate specimens is employed, as well as a multianalyzer stage featuring nine analyzer crystals. An XRD 1611CP3 flat panel detector can also be used for total scattering measurements. Further details on the ID22 beamline setup and capabilities can be found in references [41, 42]. Data treatment was performed using EVA version 7.

2.4.3 SR-μXRF

Highly sensitive SR-μXRF measurements were carried out at the PUMA beamline (SOLEIL Synchrotron Radiation Facility, France) using a 20 keV monochromatic microbeam measuring 7 μm (horizontal) x 5 μm (vertical). An optimal detection of all the elements of interest in this experiment can be achieved, from phosphorus (P) to zirconium (Zr) using the K lines, as well as lead (Pb) and bismuth (Bi) using the L lines. An SDD detector (RaySpec) with an area of 100 mm^2 collimated to 80 mm^2 is positioned at 90° with respect to the incident beam. The energy resolution of the SDD is 134 eV at 5.9 keV (Mn-Kα). The samples are mounted on a motorized X-Y stage, arranged in a 45°/45° geometry with respect to the incident beam and detector. The area to be analyzed is visualized by means of an optical video microscope camera with a 10x magnification lens and 10 μm focal depth that assures the accurate positioning of the sample. A more detailed description of the beamline can be found in [32, 43–46]. Chemical cartographies were performed on a millimetric area of the sample, with spectra collected in continuous scanning mode. The step size, acquisition time, and area of the XRF maps are presented in Table I of the SI.

The obtained dataset consists of a matrix where each pixel contains an XRF spectrum and is saved in HDF5 format. Using the PyMCA program [47], the peak area of different elements can be fitted and elemental maps in PNG format are obtained. These chemical maps are scaled to optimize readability. The PyMCA version used was 5.6.5. A correlation study of minor and trace elements present with respect to the main elements of the red iron oxide-based coloring matter (Fe), and the calcitic support, (Ca) was performed followed by a PCA statistical analysis using Orange Datamining version 3.32.0.

3 Results and discussion

3.1 Trace and minor elemental analysis of the red coloring matter

All thirteen samples were studied by SR-μXRF analysis and imaging (see SI for a detailed description of the results for each sample). One sample from drip point ALT1_1 was further analyzed using SR-XRD, which confirmed that the red coloring matter samples are generally hematite-based with a varying proportion of goethite, and therefore the search for characteristic phase differentiation criteria is not feasible. The XRD patterns that show the main mineral phase of hematite, as well as quartz and calcite, is presented in Fig. XIV of the SI.

Figure 3a displays the SR-μXRF sum spectrum of all the individual spectra from each analyzed pixel on the ALT1_4 sample. The fit of the peaks, performed with PyMCA [47], appears in red. Figure 3b-e present the chemical maps of Fe, Ca, Mn and Zn in sample ALT1_4, obtained by plotting the intensity of each element's representative peak versus the position using a linear scale. A slightly heterogeneous distribution of elements can be observed in the analyzed sample, and an initial correlation of elements can be deduced based on these images. This preliminary association will help establish the correlations discussed in the following section.

In addition to Fe, the main element in the Fe oxide-based coloring matter, a large range of elements such as P, S, Cl, K, Ti, V, Cr, Mn, Co, Cu, Zn, Pb, As, Br, Rb, Sr, Zr and Nb were detected. Ca could come from the coloring block, which naturally contains some calcium. A slight contamination with the dried calcitic contents of the water drop cannot be ruled out. The individual sum spectra for the other twelve samples are provided in the SI.

Looking at the sum spectra for all the thirteen samples under study, numerous elements appear potentially associated with Fe: Si, K, Ca, Ti, V, Cr, Mn, Co, Ni, Cu, Zn, Ga, Pb, As, Br, Rb, Sr, Y and Zr. Most of these elements are present in the sum spectra of all the samples, while K, V, Ni, Ga, As, Br and Si appear only in a few. This extensive list of elements possibly associated with the Fe-based red matter is consistent with our previous studies in caves from Northern Spain [19, 32] as well as other bibliographic references employing further methods [15, 16, 20, 48].

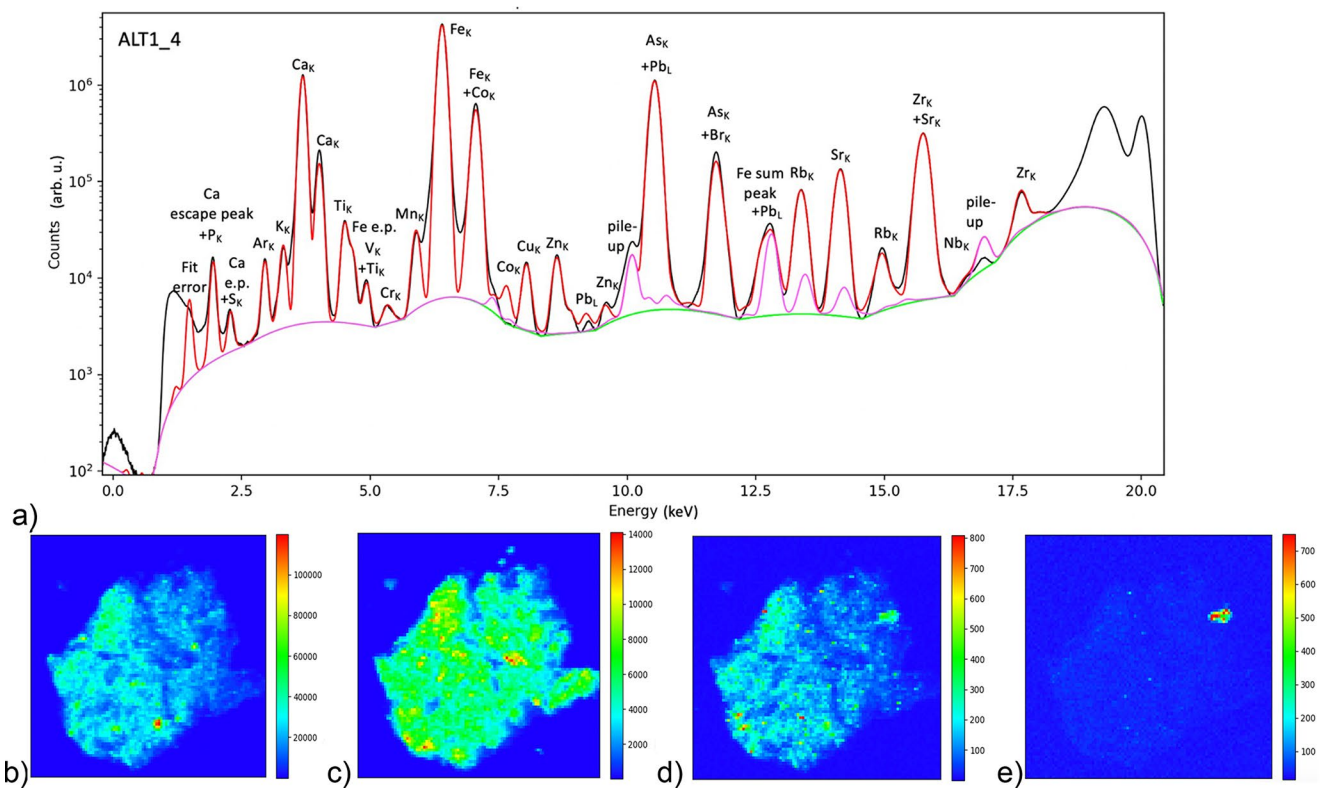

Fig. 3 **a**) SR-μXRF sum spectrum of each of the individual spectra per analyzed pixel in the studied zone (0.35 × 0.3 mm^2) of sample ALT1_4 shown in Fig. 2c. The elements are identified in the sum spectrum and, in red, is displayed its fit performed with the PyMCA program. The green and pink lines are the background of the spectrum taken into account by PyMCA when performing the fit. Scan conditions: step size 7 μm, 0.5 s/point. Corresponding chemical maps, using a linear scale, of **b**) Fe K, **c**) Ca K, **d**) Mn K, and **e**) Zn K

3.2 Correlation study of whether elements are related to the coloring matter or the support

To clarify the question of association of the minor and trace elements with the Fe oxide-based coloring matter, the correlation of the elemental intensities with that of Fe K, mainly representative of the coloring matter, and Ca K, primarily representative of the calcitic support, was performed for all the samples. As a general tendency, when the Fe intensity is high, that of Ca is low and vice versa. However, there are many points in between. The Ca-Fe correlation is complicated, as Ca can originate from multiple sources including the cave wall, but also in the block of matter used to paint the figure as Ca carbonate [11], resulting in a scatter plot of Ca K vs. Fe K intensities without a clear pattern (see the SI).

Several relevant elements were selected to display their relationship to the coloring matter, or the calcitic support or calcite from the water drops. In order to perform this intensity ratio study, for each of the thirteen samples the following procedure was repeated: from each individual spectrum obtained for every pixel of the map, the peak area of the different elements was plotted against that of Fe K and Ca K. If, under visual inspection, the intensity of an element increases with increasing Fe intensity (or Ca), it means that they are most likely correlated and the element can be associated to the red coloring matter (or calcitic support). In Fig. 4 this is shown for samples ALT1_1B and ALT12_3 for elements Mn, Rb, Pb, Co against Fe, and K and Sr against Ca. As ALT12_3 showed under the microscope particles of the calcitic support, which had apparently detached from the ceiling of the cave together with the coloring matter, it should give more representative Ca ratio results than the other samples. For ALT1_1B (Fig. 4a), Mn, Rb, Pb and Co are clearly correlated with Fe, and K with Ca. For ALT12_3 (Fig. 4b), Mn, Rb, Pb and Co appear to be correlated with Fe, and Sr with Ca. The bi-plots for all samples are presented in the SI, alongside with a table summarizing the correlations found for each sample (Table II in the SI).

As a summary of the results for all the samples, Fe, corresponding to the coloring matter, is frequently found to be correlated with Mn, Co, Rb, Zn and Pb. In some cases, also with Cu, Ti, K, Cr and Br. Calcium of the calcitic support, seems correlated with Sr and K, and in some cases with Br, Mn, Ti and Zn. This is in agreement with our previous study using CXRF and SR-μXRF on a prehistoric sample presenting red coloring matter [32], where Fe was accompanied by Mn, Zn and Co in most cases, occasionally with Ti and K, and rarely with Cr, Cu, Rb, Bi or Ga. Ca, together with Br and Sr, was occasionally correlated with Bi and Ga and rarely with K, Cl, Cu, Pb, Y, Rb or As. Additionally, these findings are also in agreement with the SR-μXRF study performed by our team on other samples from La Garma cave

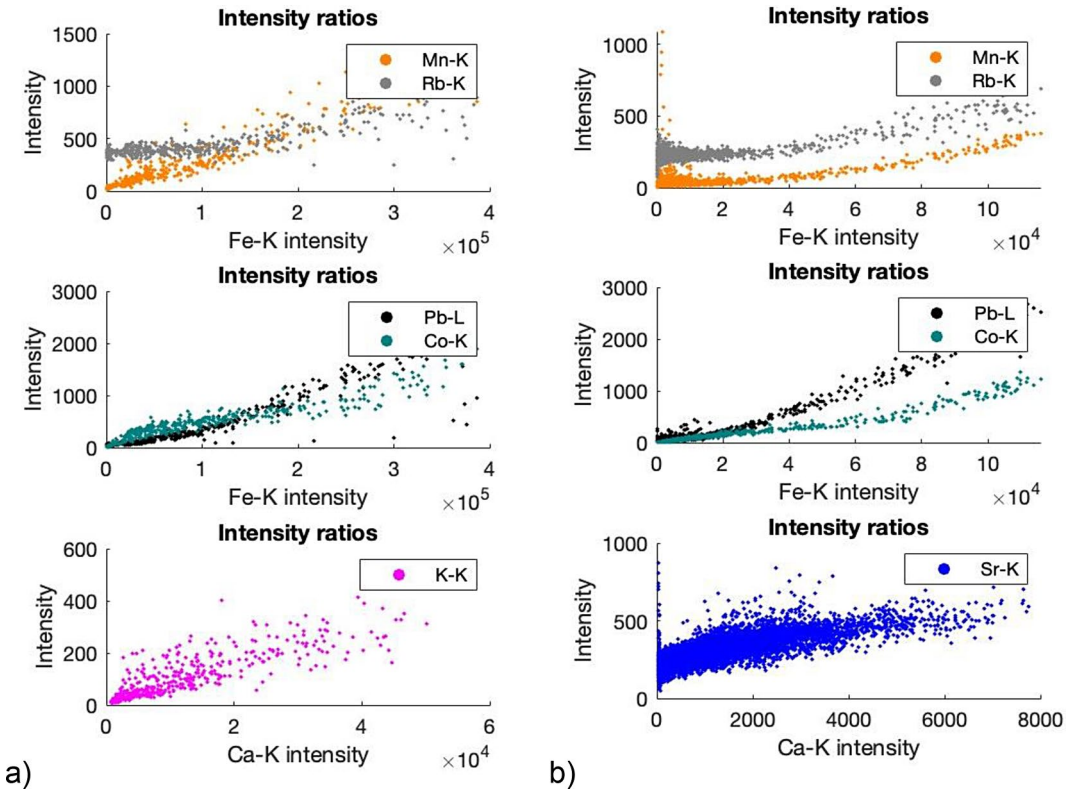

Fig. 4 Intensity of different elements plotted against the intensity of Fe K or Ca K for (**a**) ALT1_1B and (**b**) ALT12_3, to find possible correlations

in Northern Spain, where Fe, Ti and K were found associated with the red coloring matter [19].

3.3 PCA analysis and clustering of the red coloring matter studied

The statistical method of Principal Component Analysis (PCA) was applied to identify further patterns and relationships between the samples. PCA allows reducing the dimensionality of the data by means of the principal components, linear combinations of the original variables that capture the maximum variance in the data. The sum spectra of each sample were normalized to their Fe Kα peak, and the maximum intensity values of fourteen characteristic elements (namely Cl Kα, K Kα, Ti Kα, V Kα, Cr Kα, Mn Kα, Co Kβ, Cu Kα, Zn Kα, As Kα, Rb Kα, Sr Kα, Zr Kβ, and Pb Lβ) were considered for PCA computation. Several score maps were obtained and are presented in Fig. 5 (namely PC2, PC3 and PC5 against PC1). Score plot PC4 against PC1 is shown in the SI.

Several clusters were visually identified in the score plots. Marked in blue, ALT1_1A, ALT1_1B, ALT1_1C, ALT12 and ALT12_3 appear in the same cluster. The three samples from location ALT12 would be divided into two,

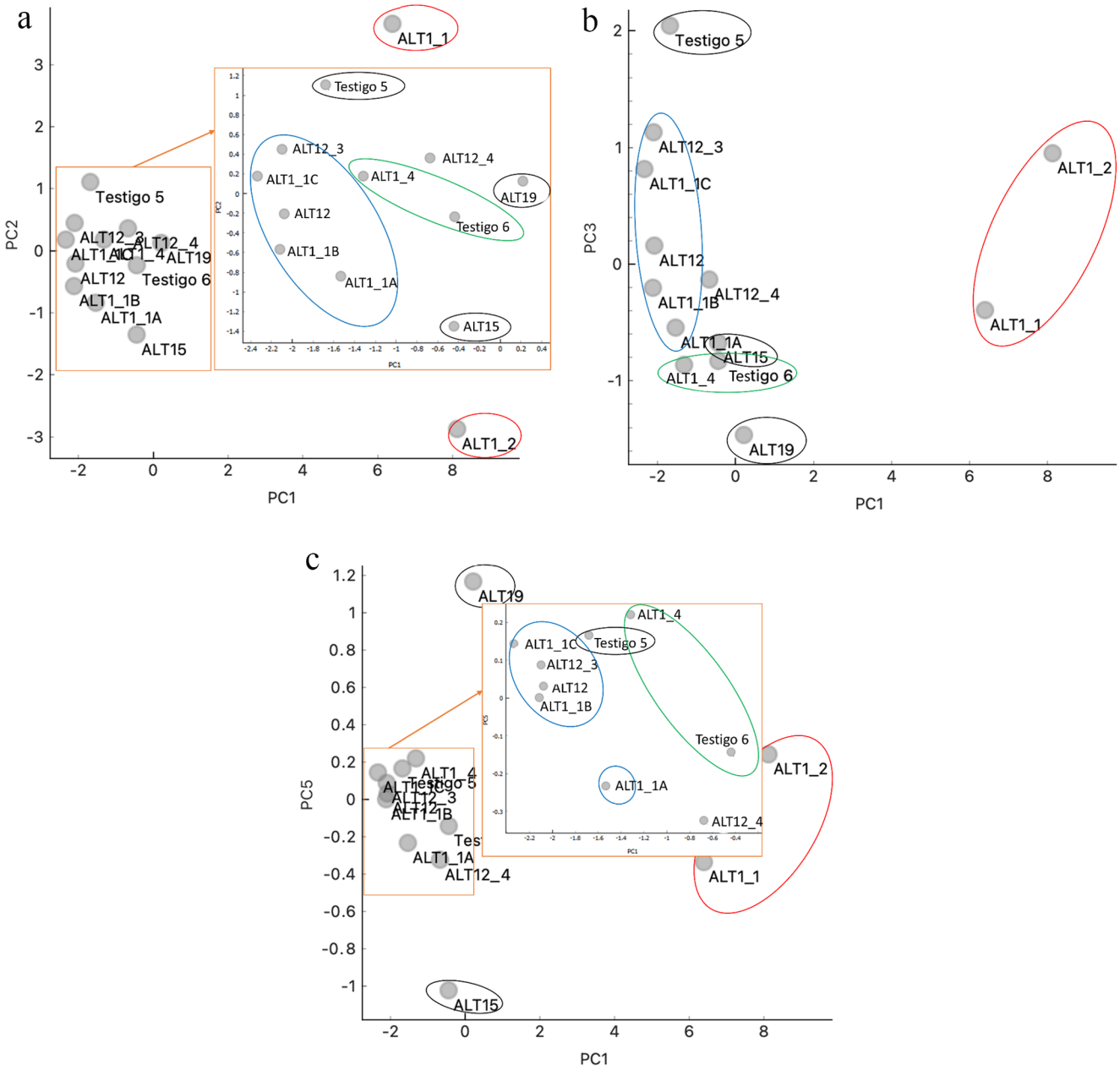

Fig. 5 Score plots of different PCAs with observed clusters marked (blue, green, red): (**a**) PC1 vs. PC2, (**b**) PC1 vs. PC3, (**c**) PC1 vs. PC5

Table 2 Overview of the PCA clusters found, the samples assigned to the individual clusters and the representation in the cave from which they originate

PCA cluster	Sample	Representation
1	ALT1_1A, ALT1_1B, ALT1_1C	Claviform sign A, in ALT1 area
	ALT12, ALT12_3	Claviform sign C
2	ALT1_1	Claviform sign A in ALT1 area
	ALT1_2	Claviform sign B(?) in ALT1 area
3	Testigo 6	Claviform sign F
	ALT1_4(?)	Superposition of claviform signs A and B in ALT1 area
Independent	ALT15	Claviform sign D
	ALT19	Polychrome bison
	Testigo 5	Claviform sign E

ALT12 and ALT12_3 in the blue cluster, and ALT12_4 on its own. ALT1_1 and ALT1_2 appear in a second red cluster, clearly different from the others but with enough similarities to remain together rather than in separate clusters. A third green cluster might exist, consisting of ALT1_4 and Testigo 6. ALT19 appears separated from the rest, as so do ALT15 and Testigo 5, and are marked in black. Table 2 lists all the samples, the figures to which they belong, and the groups they were accorded in the PCA analysis.

3.4 Comparison of normalized spectra with respect to PCA groups

Further comparisons are presented in Figs. 6 and 7 to complement the PCA results. The sum spectra of several samples, normalized to their Fe Kα peak, are compared. Given the precision and level of detail obtained with SR-μXRF analyses, strong similarities between sum spectra would indicate that the same coloring matter is present in the samples in question, as slightly different matters would show clear spectral differences. Characterizing features were

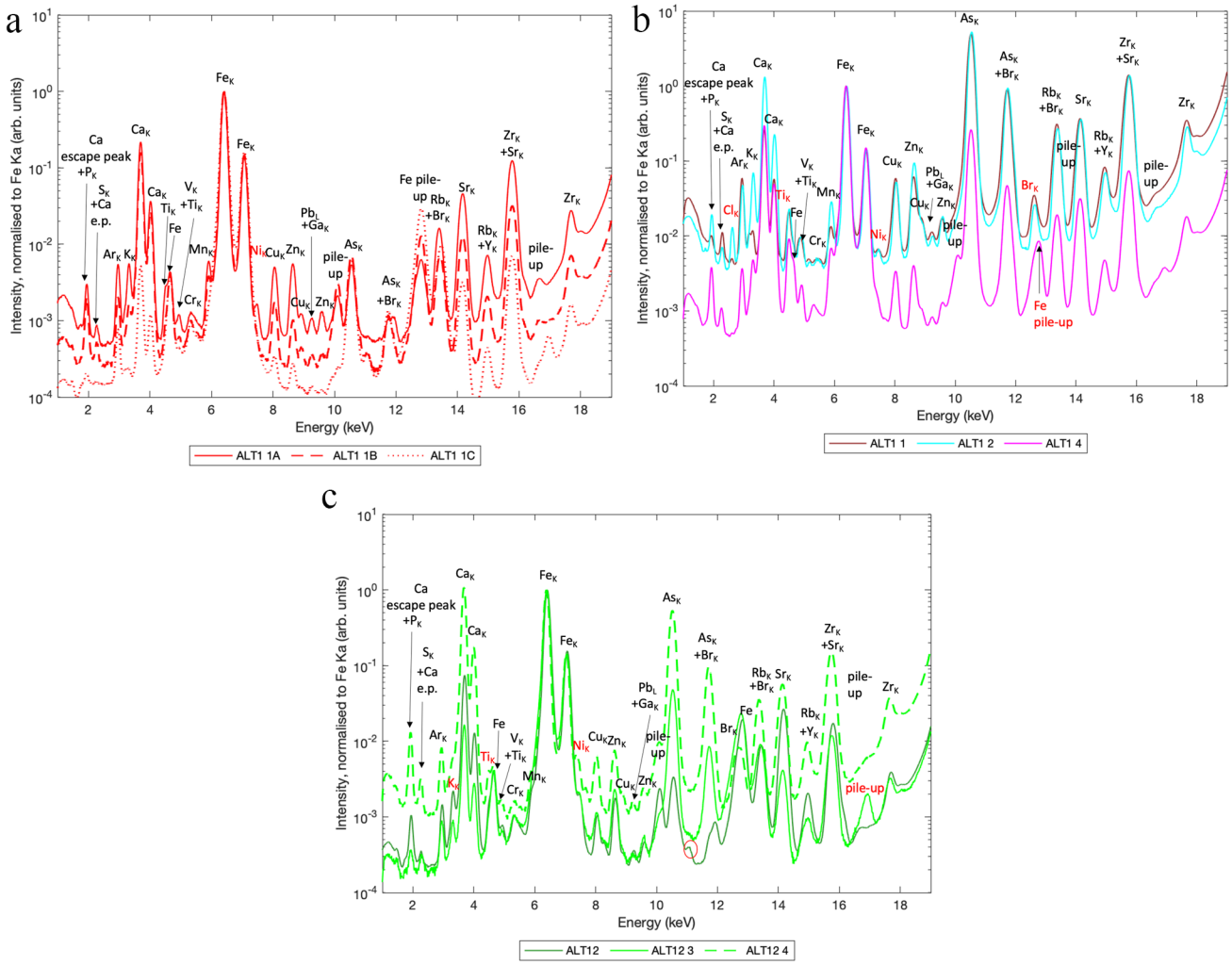

Fig. 6 Comparison of the sum spectra of the samples, normalized to the Fe Kα peak, with the characterizing differences arising marked in red, of: (**a**) ALT1_1A, ALT1_1B, ALT1_1C, from drip point ALT1_1 (**b**) ALT1_1, ALT1_2 and ALT1_4, from two claviform signs within the ALT1 area, (**c**) ALT12, ALT12_3 and ALT12_4, from drip point ALT12

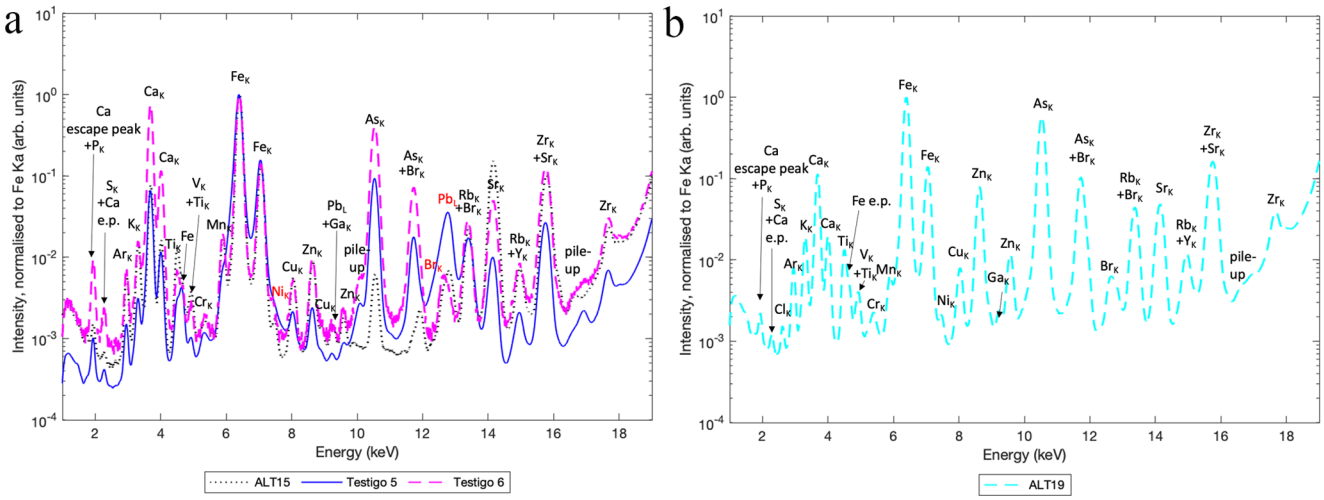

Fig. 7 Comparison of the sum spectra of the samples, normalized to the Fe Kα peak, with the characterizing differences arising marked in red, of: (**a**) ALT15, Testigo 5 and Testigo 6, from three different signs close to each other, (**b**) ALT19, from a polychrome bison

identified and used to differentiate the sum spectra, such as the Ca and Fe content and the presence or absence of Cl, K, Ti, Ni, Co and Pb, to name a few.

3.4.1 Chemical homo- or heterogeneity of the samples coming from claviform signs

Figure 6a compares the sum spectra of three samples from drip point ALT1_1, in claviform A. The sum spectrum of ALT1_1A presents the same characterizing features as ALT1_1B. The sum spectrum of ALT1_1B is also very similar, although not identical, to that of ALT1_1C. These three samples were grouped together in the blue cluster in the PCA analysis (first group), and the spectra comparison agrees with it.

Figure 6b displays the sum spectra of three samples from the three drip points (d.p. ALT1_1, ALT1_2 and ALT1_4), belonging to the two claviforms (A and B) in area ALT1. Sample ALT1_1 is expected to contain exclusively coloring matter from claviform A, sample ALT1_4 matter from the superposition of both signs, and ALT1_2 either matter from the superposition or solely from claviform B. The sum spectra of samples ALT1_1 and ALT1_2 are almost identical, which could be due to a lower Fe content in these samples, perhaps owing to the fact that they were taken chronologically after the other samples when the color was already washed out. Despite of this color washing, it could also be possible that the same coloring matter is present in both samples. As identifying features, their spectra presents particularly a higher Cl and Br peak intensities. The two samples were found in the PCA analysis as a possible second group separated from the rest (red cluster). ALT1_4, on the other hand, presents spectral features that confirm its belonging to a different group (green cluster in the PCA). This sample should be considered on its own, since its coloring matter stems from the superposition of two figures.

Figure 6c shows the sum spectra of three samples (ALT12, ALT12_3 and ALT12_4) from the same drip point in claviform sign C (d.p. ALT12). The spectra of samples ALT12 and ALT12_3 are almost identical. The two present small differences with the spectra of ALT12_4, although most of the important characterizing features are shared between these samples. The divergences might be due to the fact that sample ALT12_4 was recovered in 2014, almost ten years prior to the other two. In addition, as determined by optical microscopy, samples ALT12 and ALT12_3 contain some minuscule black and white grains that may have slightly altered their chemical composition. Another possible explanation to the differences would be the natural heterogeneity inside of the coloring matter block, which would make different samples of the same figure to slightly differ chemically. Looking at the PCA study, sample ALT12_4 had been established to stand on its own, while samples ALT12 and ALT12_3 belonged to the first group (blue cluster).

Figure 7a presents the sum spectra of samples ALT15, Testigo 5 and Testigo 6, coming from drip locations in three different claviform signs that are very close to each other (claviforms D, E, F). Clear differences emerge between their sum spectra, making it impossible to group any of them together, even though it was expected that the same coloring matter might have been used in at least two, given the proximity of the signs within the cave. In the PCA analyses, no clear groupings were found for samples ALT15 and Testigo 5, while Testigo 6 could perhaps be placed in the third group (green cluster) with ALT1_4. However, since ALT1_4 likely comes from a mix of coloring matter, a clear conclusion cannot be drawn. The differences between the spectra of ALT15, Testigo 5 and Testigo 6 observed by the

PCA are therefore confirmed by the spectral comparison in Fig. 7a.

3.4.2 Chemical signature of the bison sample (ALT 19)

Figure 7b displays the spectrum of ALT19, which comes from a drip point in a polychrome bison. The sum spectrum of this sample does not show clear similarities with that of other samples, only slightly with that of Testigo 6, but not enough to group them together. The PCA analysis showed that ALT19 appears separated from the rest, and this could indeed be confirmed by comparing the spectra. For further comparison, the reader is invited to observe the individual spectra presented in the SI.

3.4.3 Possible conclusions in relation to application scenarios of the prehistoric figures

From these results, preliminary suppositions regarding the creation steps of the figures can be made. The coloring matter from the claviform sign A, containing the drip point ALT1_1, might also have been used in another figure a few meters away, the sign C to which the drip point ALT12 belongs to. It was assumed that samples ALT1_1 and ALT1_2 have an almost identical sum spectra due to a washout of the color at the drip point. However, it cannot be ruled out that the same coloring matter is present in both samples, as their drip points are only a few centimeters apart. Sample ALT1_4 is clearly different from all the four samples from a similar location, supporting the idea that the two superposing figures were likely painted using two different coloring matters and consequently were not completed at the same time.

Samples ALT_15, Testigo 5, and Testigo 6, despite coming from drip points within different signs close to each other, exhibit notable chemical differences between them. Therefore, they are likely made with different coloring matters, possibly by separate hands and/or at a different moment.

Sample ALT19, from a drip point in a polychrome bison, presents some similarities with the coloring matter of two other signs, but also clear chemical differences not allowing to establish direct relations. This is not unexpected, as the bison was painted with a different technique and its color tends to be browner than the otherwise red samples analyzed elsewhere. Further analyses are necessary in order to clarify the possible application scenarios.

4 Conclusions

The high sensitivity of SR-μXRF allowed for a detailed characterization and distinction of the red coloring matter from different figures of the *Techo de los Polícromos* in the Altamira cave. Looking at the sum spectra, a large range of elements, namely Si, K, Ti, V, Cr, Mn, Co, Ni, Cu, Zn, Ga, Pb, As, Br, Rb, Sr, Y and Zr, was found to be possibly related with the red Fe-based coloring matter. These trace and minor elements are in agreement with results by other authors, a previous SR-μXRF study on La Garma cave by members of our team, and our combined SR-μXRF and CXRF study of a prehistoric stalactite presenting red coloring matter. These characteristic elements enable comparisons between figures and can guide future in situ analyses in Paleolithic caves.

The study of the intensity ratio correlation of several elements with that of Fe K and Ca K indicated that the Fe-based coloring matter is likely to contain Mn, Co, Rb, Zn and Pb, and sometimes Cu, Ti, K, Cr and Br. The calcitic support (Ca), even if little present due to the nature of the samples, would likely be correlated with Sr and K, and occasionally with Br, Mn, Ti and Zn. Based on the current study, we are unable to make an assessment regarding the origin or associations of the elements Si, V, Cr, Ga, As or Zr. These findings are in agreement with our previous CXRF study that separated the red Paleolithic coloring matter layer from its calcitic support, and can aid in future on-site campaigns.

Comparisons and groupings of coloring matter and figures were found in the Altamira cave. A first group would include samples from two different claviform signs (drip points ALT1_1 and ALT12). The same coloring matter of the claviform sign A (d.p. ALT1_1) was probably employed in another sign situated a few meters away (sign C, d.p. ALT12). A second group would consist of two samples showing a nearly identical spectra (samples ALT1_1 and ALT1_2). A third group could include samples from two distant signs (d.p. ALT1_4, Testigo 6), but further analyses are required to confirm this association. This group might also include a polychrome bison (d.p. ALT19), although the latter might, more likely, be considered independently. Three signs located very close to each other (d.p. ALT15, Testigo 5 and Testigo 6) unexpectedly appear to not be associated between them. It is therefore likely that they were made with different red coloring matters, likely executed by separate hands or at different moments. These results demonstrate the efficacy and power of SR-μXRF studies to group, compare and correlate figures in a way not achievable using in situ methods. Finally, the results obtained here will help future studies, namely in situ with pXRF.

Samples of dried drops without coloring matter were not available for this study. They should be sampled and analyzed by SR-μXRF in the future to be used as references and to confirm the assumption that our results are not significantly affected by the calcium carbonate present in the drops that detach the coloring matter. Moreover, with the results presented here, a pigment provenance study could be envisioned in the future. Furthermore, by analyzing red coloring matter samples from other caves in Northern Spain using SR-μXRF, the decoration

of different Paleolithic cave sites could be compared in a future work, offering a broader understanding of the use of red coloring matter on a regional scale.

Supplementary Information The online version contains supplementary material available at https://doi.org/10.1007/s00339-024-07950-5.

Acknowledgements We thank Clément de Mecquenem from the C2RMF laboratory for his help with the PCA data treatment. We further thank Catherine Dejoie, Marine Cotte, Clément Holé and Lise Boutenegre for their assistance with the XRD measurements at the ID22 beamline of the ESRF (European Synchrotron Radiation Facility), Historical Materials BAG (Block Allocation Group) Access, experiment HG213 (February 2024). The research presented in this manuscript was conducted as part of the PrehMIND project (PID 2020-112832RB-100) funded by the Spanish Ministry of Science and Innovation and directed by P.A. SR-µXRF analyses were performed in November 2022 and October 2023 at the PUMA line, SOLEIL synchrotron, under programs n° 20220332 and nº 20230520 directed by J.T. Analyses and sampling partly funded by the ANR DepthPaint project (ANR-20-CE29-0018).

Author contributions The manuscript was written through contributions of J.T., I.R. and K.M. All authors have contributed to the data acquisition. All authors have given approval to the final version of the manuscript.

Funding Open Access funding provided thanks to the CRUE-CSIC agreement with Springer Nature.

Data availability The data produced in this study is available upon request to the corresponding author. The optical micrographs, sum XRF spectra, elemental mappings, and elemental intensity ratios correlation of the thirteen samples studied are either included in the manuscript or provided in the SI.

Declarations

Conflict of interest There is no conflict of interest to declare.

References

1. A. Leroi-Gourhan, *Préhistoire de l'Art Occidental.* Mazenod Paris (1965).
2. A. Leroi-Gourhan (ed.), *Lascaux Inconnu. Gallia préhistoire Supplément*, Vol. 12, (CNRS, Paris, 1979)
3. C. Vignaud, H. Salomon, E. Chalmin, J.-M. Geneste, M. Menu, Le groupe des « bisons adossés » de Lascaux. Étude de la technique de l'artiste par analyse des pigments, *L'Anthropologie*. **110**(4), 482–499 (2006). https://doi.org/10.1016/j.anthro.2006.07.008
4. D. Genty et al., Datations U/Th (TIMS) et 14 C (AMS) des stalagmites de la grotte Chauvet (Ardèche, France): intérêt pour la chronologie des événements naturels et anthropiques de la grotte, Comptes Rendus Palevol. **3**(8), 629–642 (2004). https://doi.org/10.1016/j.crpv.2004.06.005
5. J. Clottes (ed.), Return to Chauvet Cave: excavating the birthplace of art: the first full report. (Thames & Hudson, London, 2003). Available: https://search.worldcat.org/fr/title/56438470
6. M. Gay, F. Plassard, K. Müller, I. Reiche, Relative chronology of palaeolithic drawings of the great ceiling, Rouffignac cave, by chemical, stylistic and superimposition studies. J. Archaeol. Sci. Rep. **29**, 102006 (2020). https://doi.org/10.1016/j.jasrep.2019.102006
7. T. Martin-Pozas et al., Microclimate, airborne particles, and microbiological monitoring protocol for conservation of rock-art caves: the case of the world-heritage site La Garma cave (Spain). J. Environ. Manage. **351**, 119762 (2024). https://doi.org/10.1016/j.jenvman.2023.119762
8. M. Lorblanchet, Art pariétal: grottes ornées du Quercy. Antiquity. **86**(332), 573–574 (2010). https://doi.org/10.1017/S0003598X00063018
9. M. Menu, L'analyse de l'art préhistorique. L'Anthropologie **13**(3), 547–558 (2009). https://doi.org/10.1016/j.anthro.2009.09.011
10. I. Reiche, A. Trosseau, K. Müller, M. Gay, D. Strivay, J.-J. Cleyet-Merle, Analyses non invasives in situ des œuvres préhistoriques de la grotte de Font-de-Gaume pour une meilleure connaissance du décor pariétal polychrome et de son organisation, PALEO Rev. Archéologie Préhistorique. **30**(2), 262–269 (2020). https://doi.org/10.4000/paleo.5707
11. J. M. Cabrera Garrido, Les matériaux de peinture de la Caverne d'Altamira Proc. ICOM Committee for Conservation 5th Triennial Meeting, Zagreb, Yugoslavia, 113 (1978)
12. O. Ballet, A. Bocquet, R. Bouchez, J.M.D. Coey, A. Cornu, Etude technique des poudres colorées de Lascaux, in: *Lascaux Inconnu*, A. Leroi-Gourhan (ed.)171–174 (1979)
13. P. Vandiver, *Paleolithic pigments and processing*. Thesis (M.S.), Massachusetts Institute of Technology, Dept. of Materials Science and Engineering (1983). http://hdl.handle.net/1721.1/15514
14. B.H. Stuart, P.S. Thomas, Pigment characterisation in Australian rock art: a review of modern instrumental methods of analysis. Herit. Sci. **5**(1), 10 (2017). https://doi.org/10.1186/s40494-017-0123-8
15. E.C. Velliky, B.L. MacDonald, M. Porr, N.J. Conard, First large-scale provenance study of pigments reveals new complex behavioural patterns during the Upper Palaeolithic of south-western Germany. Archaeometry. **63**(1), 173–193 (2021). https://doi.org/10.1111/arcm.12611
16. L. Dayet, F.-X.L. Bourdonnec, F. Daniel, G.E. Porraz, P.-J. Texier, Ochre provenance and procurement strategies during the middle stone age at Diepkloof Rock Shelter, South Africa. Archaeometry. **58**(5), 807 (2016). https://doi.org/10.1111/arcm.12202
17. A. Chieli,M. Vendrell,C. Roldán,P. Giráldez, I. Domingo, Characterizing paint technologies and recipes in Levantine and Schematic rock art: El Carche site as a case study (Jalance, Spain). PLOS ONE. **17**(8), e0271276 (2022). https://doi.org/10.1371/journal.pone.0271276
18. E. Chalmin, I. Reiche, X.-R. Synchrotron, Microanalysis and Imaging of Synthetic Biological Calcium Carbonate in Comparison With Archaeological Samples Originating from the Large Cave of Arcy-sur-Cure (28000–24500 BP, Yonne, France). Microsc. Microanal. **19**(6), 1523–1534 (2013). https://doi.org/10.1017/S1431927613013342

19. M. Gay et al., Palaeolithic paint palettes used at La Garma Cave (Cantabria, Spain) investigated by means of combined in situ and synchrotron X-ray analytical methods. J. Anal. Spectrom. **30**(3), 767–776 (2015). https://doi.org/10.1039/C4JA00396A
20. H. Salomon et al., Stratégies spécialisées d'acquisition de pigments rouges durant le Châtelperronien de la grotte du Renne à Arcy-sur-Cure (Yonne, France), PALEO *Actes Colloq. « Micro-Anal. Datations Art Préhistorique Dans Son Contexte Archéologique » MADAPCA - Paris, 16–18 Novembre 2011 (ed. P. Paillet)*, **numéro sp.**, 125–133 (2014)
21. T. Trojek, R. Prokeš, R. Šefců, H. Bilavčíková, T. Čechák, Confocal X-ray fluorescence spectrometer for in-situ analyses of paintings. Radiat. Phys. Chem. **137**, 238–242 (2017). https://doi.org/10.1016/j.radphyschem.2016.02.031
22. E. Ravaud, L. Pichon, E. Laval, V. Gonzalez, M. Eveno, T. Calligaro, Development of a versatile XRF scanner for the elemental imaging of paintworks. Appl. Phys. A. **122**(1), 17 (2016). https://doi.org/10.1007/s00339-015-9522-4
23. M. Eveno, E. Mysak, K. Müller, G. Bastian, N. Pincas, I. Reiche, Confocal XRF depth profiling non-destructively reveals the original blue pigments in a Renaissance painting by Caroto. Stud. Conserv. **61**, 102–112 (2016). https://doi.org/10.1080/00393630.2016.1142059
24. P. Arias, E. Laval, M. Menu, C.G. Sainz, R. Ontañón, Les colorants dans l'art pariétal et mobilier paléolithique de La Garma (Cantabrie, Espagne). L'Anthropologie **115**(3-4), 425–445 (2011). https://doi.org/10.1016/j.anthro.2011.05.005
25. I. Reiche, C. Vignaud, É. Chalmin, M. Menu, J.-M. Geneste, The ornamentation steps of the Bull Rotunda of the Lascaux cave give new insights into the Upper Paleolithic natural life cycle. Archaeometry. **66**(4), 877–893 (2024). https://doi.org/10.1111/arcm.12960
26. A. Trosseau, Caractérisation physico-chimique in situ des matières colorantes à base d'oxydes de fer et de manganèse des parois des grottes ornées, ex. Font-de-Gaume (France). https://pastel.hal.science/tel-04026840
27. C. Roldán et al., Application of field portable EDXRF spectrometry to analysis of pigments of levantine rock art. X-Ray Spectrom. **39**(3), 243–250 (2010). https://doi.org/10.1002/xrs.1254
28. L. Beck et al., In situ analysis of rock art in the cave of Rouffignac by using a portable XRF-XRD system. Archéo Sci. **36**(1), 139–152 (2012).
29. A.W.G. Pike et al., U-series dating of paleolithic art in 11 caves in Spain. Science. **336**(6087), 1409–1413 (2012). https://doi.org/10.1126/science.1219957
30. C. De Las Heras Martin, J.A. Lasheras Corruchaga, Altamira cave, in *Pleistocene and Holocene hunter-gatherers in Iberia and the Gibraltar Strait. The Current Archaeological Record*, ed. by R. Salas Ramos (Burgos: Fundación Atapuerca, 2014), p. 615–627.
31. L. Blas, España. Cuevas De Altamira,*Patrimonio De La Humanidad. Europa Mediterránea*, UNESCO/Planeta DeAgostini/Ediciones San Marcos, 34–37 (1999)
32. J. Tapia et al., Improving the characterization of red coloring matter from prehistoric cave art by means of confocal XRF depth profiling combined with synchrotron XRF imaging. J. Cult. Herit. **67**, 385–394 (2024). https://doi.org/10.1016/j.culher.2024.03.018
33. A. Trosseau, Y. Coquinot, I. Reiche, An improved method for characterizing red rock art by extracting and extrapolating element intensities of the coloring matter in p-XRF spectra: XRF-TESIE. J. Archaeol. Sci. submitted
34. P. Martín-Ramos, J.A. Cuchí-Oterino, M. Bea-Martínez, Portable X-ray fluorescence analysis of levantine and schematic art pigments from the River Vero shelters (Huesca, NE Spain. Heritage. **6**(4), 3789–3800 (2023). https://doi.org/10.3390/heritage6040201
35. C. Chanteraud et al., Contribution and limits of portable X-ray fluorescence for studying Palaeolithic rock art: a case study at the points cave (Aiguèze, Gard, France). J. Archaeol. Sci. Rep. **37**, 102898 (2021). https://doi.org/10.1016/j.jasrep.2021.102898
36. L. Dayet, F. d'Errico, M. García Diez, J. Zilhão, Critical evaluation of in situ analyses for the characterisation of red pigments in rock paintings: a case study from El Castillo, Spain. PLOS ONE. **17**(1), e0262143 (2022). https://doi.org/10.1371/journal.pone.0262143
37. V. Bayarri, A. Prada, F. García, C. De Las Heras, P. Fatás, Remote sensing and environmental monitoring analysis of pigment migrations in cave of Altamira's prehistoric paintings. Remote Sens. **16**(12), 2099 (2024). https://doi.org/10.3390/rs16122099
38. V. Bayarri, A. Prada, F. García, C. De Las Heras, P. Fatás, A multisensory analysis of the moisture course of the Cave of Altamira (Spain): implications for its conservation. Remote Sens. **16**(1), 197 (2024). https://doi.org/10.3390/rs16010197
39. J.-H. Jang, B.A. Dempsey, W.D. Burgos, Solubility of hematite revisited: effects of hydration.Environ. Sci. Technol. **41**(21), 7303–7308 (2007). https://doi.org/10.1021/es070535t
40. M. Cotte et al., The 'Historical materials BAG': a new facilitated access to synchrotron X-ray diffraction analyses for cultural heritage materials at the European synchrotron radiation facility. Molecules. **27**(6), 1997 (2022). https://doi.org/10.3390/molecules27061997
41. J.-L. Hodeau, P. Bordet, M. Anne, A. Prat, A. N. Fitch, E. Dooryhee, G. Vaughan, A. K. Freund, Nine-crystal multianalyzer stage for high-resolution powder diffraction between 6 keV and 40 keV. SPIE Proc. Crystal Multilayer Opt. **3448**, 353–361 (1998). https://doi.org/10.1117/12.332525
42. J. Wright, G.B.M. Vaughan, A. Fitch, Merging data from a multidetector continuous scanning powder diffraction system. International Union of Crystallography Commission on Crystallographic Computing Newsletter. **1**, 92–96 (2003)
43. A. Gianoncelli et al., Synchrotron μ-XRF imaging and μ-XANES of black-glazed wares at the PUMA beamline: insights on technological markers for colonial productions. Microchem J. **154**, 104629 (2020). https://doi.org/10.1016/j.microc.2020.104629
44. P. Tack et al., Investigation of (micro-)meteoritic materials at the new hard X-ray imaging PUMA beamline for heritage sciences. J. Synchrotron Radiat. **26**(6), 2033–2039 (2019). https://doi.org/10.1107/S160057751901230X
45. L. Tranchant et al., Improved discrimination of biogenic and diagenetic elements in Palaeolithic mammoth ivory and bone from Hohle Fels Cave in the Swabian Jura of Southwestern Germany. Quat. Int. **660**, 4–12 (2023). https://doi.org/10.1016/j.quaint.2023.02.006
46. L. Tranchant et al., Performance comparison of external IBA and SR-XRF imaging for the study of ivory. NIMB **545**, 165146 (2023). https://doi.org/10.1016/j.nimb.2023.165146
47. V.A. Solé, E. Papillon, M. Cotte, P. Walter, J. Susini, A multiplatform code for the analysis of energy-dispersive X-ray fluorescence spectra. Spectrochim Acta Part. B Spectrosc. **62**, 63–68 (2007)
48. R.S. Popelka-Filcoff et al., Microelemental characterisation of Aboriginal Australian natural Fe oxide pigments. Anal. Methods. **7**(17), 7363–7380 (2015). https://doi.org/10.1039/C5AY01547B